Progress In Electromagnetics Research, PIER 80, 307–320, 2008

MICROWAVE/MILLIMETER-WAVE GENERATION USING MULTI-WAVELENGTH PHOTONIC CRYSTAL FIBER BRILLOUIN LASER

G. F. Shen, X. M. Zhang, H. Chi, and X. F. Jin

Department of Information Science and Electronic Engineering
and The Electromagnetics Academy at Zhejiang University
Zhejiang University
Hangzhou 310027, China

Abstract—An all-optical microwave generation using a multi-wavelength photonic crystal fiber Brillouin laser is presented. A highly nonlinear photonic crystal fiber with the length of 25 m is used as Brillouin gain medium. A Fabry-Perot cavity with two fiber Bragg gratings as reflectors are designed in order to enhance the Brillouin conversion efficiency. The fiber Bragg gratings can be used to selectively excite the jth-order Stokes' wave and suppress other order Stokes' waves. The mechanism for microwave/millimeter-wave generation is theoretically analyzed. In the experiment, both 9.788 GHz and 19.579 GHz microwave signals are achieved through mixing the pump wave with the first-order and the second-order Stokes' waves.

1. INTRODUCTION

Microwave/millimeter-wave plays a more and more important role in wireless and satellite communications [1, 2]. Other applications like its materials permeability [3], imaging for iatrology [4] and industrial composites processing [5, 6] are also developing. So a good source is very necessary. Recently the way to generate microwave/millimeter-wave signals using photonics has attract lots of interest because of its high speed, low cost and high reliability [7]. Solutions for using large linewidth lasers to generate millimeter-wave with desired spectral purity was mentioned in [8, 9]. Heterodyning the outputs from two coherent oscillating continuous-wave lasers is one of the most advantageous techniques [10], it has high efficiency and the frequency range that can be generated is only limited by the bandwidth of

the photodetector. A high repetition rate picosecond pulse train is implemented in [11]. Several different hererodyning techniques for microwave/millimeter-wave generation have been reported using single-frequency laser with Mach-Zehnder-based multiplying or multi-wavelength laser [12–14]. An architecture for millimeter-wave using a fiber-grating-based dual-wavelength orthogonal polarization DFB laser was demonstrated in [15]. Four-wave mixing in a dispersion-shifted was used for yielding comb-like spectra in [16], and a rational harmonic fiber ring laser was successfully constructed in [17]. Other system, such as using a dual-wavelength single-longitudinal-mode fiber ring laser with phase-shifted fiber bragg gatings, was also employed to generate microwave [18].

There's also an increasing interest in generating microwave/millimeter-wave based on stimulated Brillouin scattering. In [19], millimeter wave was generated based on stimulated Brillouin scattering in an optical fiber and the creation of harmonics by double sideband suppressed carrier modulation. Several ways used a Brillouin fiber laser for microwave generation [20, 21]. A two frequency fiber Bragg grating-based Brillouin laser fiber with single mode fiber as the Brillouin gain medium was utilized in [22], and 11 GHz microwave signal was attained and used in radio over fiber links [23].

Recently photonic crystal fiber technique has been developed rapidly [24, 25]. Photonic crystal fiber confines small core area with single-mode behaviour over a wide wavelength range, and its high nonlinear characteristic makes it useful as stimulated Brillouin scattering gain medium. A Brillouin laser with photonic crystal fiber has also been presented [26]. In [26] a laser with holey fiber of 100 m reached threshold for a pump power of 63 mW, and it tends to produce high-order Stokes waves.

In this paper, we present a multi-wavelength fiber Bragg grating-based Brillouin laser for microwave generation by mixing the pump wave with the high-order Stokes' wave. Photonic crystal fiber is used here for its better nonlinearity. Theoretically, Fabry-Perot cavity using fiber grating pair may have arbitrary cavity length. Therefore, stable stimulated Brillouin scattering output could be realized using fiber Bragg grating-based Fabry-Perot cavity. The Brillouin frequency shift here in photonic crystal fiber is about 9.8 GHz, and the Brillouin laser performs a good stability. Experimental demonstration shows that both 9.788 GHz and 19.579 GHz microwave signals are attained.

2. THEORETICAL ANALYSIS

Stimulated Brillouin scattering is a well-known nonlinear effect in optical fiber [27–29]. It results from the interaction among a pump wave, an acoustic wave and a Stokes' wave. The frequency of Stokes' wave is downshifted from the pump wave by the Brillouin frequency f_B. The frequency difference (about $j \times 9.8\,\mathrm{GHz}$ in a 1550 nm input pump wave in the photonic crystal fiber) between the jth-order Stokes' wave and the pump wave falls in the microwave/millimeter-wave range.

The system consists of a fiber Fabry-Perot cavity closed by two fiber Bragg gratings (FBG1 and FBG2), as shown in Fig. 1. When the input optical pump power launched into the fiber Fabry-Perot cavity exceeds the Brillouin threshold, stimulated Brillouin scattering occurs. Based on the mechanism of stimulated Brillouin scattering, the pump wave (optical frequency f_p) injected into the photonic crystal fiber generates an acoustic grating moving in the direction of pump wave, which gives rise to backscattering of the optical pump (so-called the first-order Stokes' wave at f_s). The first-order Stokes' wave is frequency-downshifted from pump by f_B. Here in the fiber Fabry-Perot cavity, when the pump is strong enough, the first-order Stokes' wave may reach the threshold and generates the second-order Stokes' wave. The second-order Stokes' wave also may excite the third-order Stokes' wave, and so on.

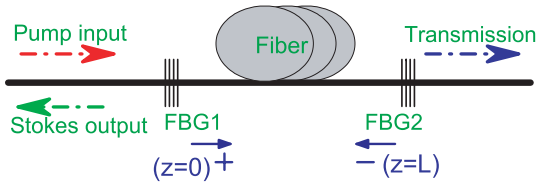

Figure 1. Schematic setup of the photonic crystal fiber Brillouin laser using Fabry-Perot cavity.

Theoretically we can get the Nth-order Stokes' wave. If only considering the first-oder and the second-order Stokes' waves, and neglecting the phase of each wave in the coupled-amplitude equations, we obtain the following coupled-power equations [22, 30]:

$$\frac{\partial P_p^{\pm}(z)}{\partial z} = \mp\alpha P_p^{\pm}(z) \mp \frac{g_B P_{s1}^{\mp}(z) P_p^{\pm}(z)}{A_{eff}} \tag{1}$$

$$\frac{\partial P_{s1}^{\pm}(z)}{\partial z} = \mp\alpha P_{s1}^{\pm}(z) \pm \frac{g_B (P_p^{\mp}(z) - P_{s2}^{\mp}(z)) P_{s1}^{\pm}(z)}{A_{eff}} \tag{2}$$

$$\frac{\partial P_{s2}^{\pm}(z)}{\partial z} = \mp\alpha P_{s2}^{\pm}(z) \pm \frac{g_B P_{s1}^{\mp}(z) P_{s2}^{\pm}(z)}{A_{eff}} \tag{3}$$

where $P_p(z)$, $P_{s1}(z)$ and $P_{s2}(z)$ are the power of the pump, and the first-order and the second-order Stokes' waves, respectively. The superscripts $\pm$ represent the direction of propagation in Fig. 1. g_B, α and A_{eff} are the Brillouin gain coefficient, the attenuation coefficient and the effective core area of the photonic crystal fiber, respectively. The boundary conditions for the equations of (1)–(3) at the input ($z = 0$) and output ($z = L$) fiber Bragg gratings are given by:

$$P_p^+(0) = (1 - R_{p0})P_{in} + R_{p0}P_p^-(0) \tag{4}$$
$$P_{s1}^+(0) = R_{s10}P_{s1}^-(0) \tag{5}$$
$$P_{s2}^+(0) = R_{s20}P_{s2}^-(0) \tag{6}$$
$$P_p^-(L) = R(pL)P_p^+(L) \tag{7}$$
$$P_{s1}^-(L) = R_{s1L}P_{s1}^+(L) \tag{8}$$
$$P_{s2}^-(L) = R_{s2L}P_{s2}^+(L) \tag{9}$$

where P_{in} is the input power. R_{p0}, R_{s10} and R_{s20} are the reflectivities of FBG1, while R_{pL}, R_{s1L} and R_{s2L} are the reflectivities of FBG2 at the wavelengths of pump wave, the first-order and the second-order Stokes' waves, respectively. The reflected and transmitted powers of the pump and the Stokes's waves are given as follows:

$$P_p^r = R_{p0}P_{in} + (1 - R_{p0})P_p^-(0) \tag{10}$$
$$P_{s1}^r = (1 - R_{s10})P_{s1}^-(0) \tag{11}$$
$$P_{s2}^r = (1 - R_{s20})P_{s2}^-(0) \tag{12}$$
$$P_p^t = (1 - R_{pL})P_p^+(L) \tag{13}$$
$$P_{s1}^t = (1 - R_{s1L})P_{s1}^+(L) \tag{14}$$
$$P_{s2}^t = (1 - R_{s2L})P_{s2}^+(L) \tag{15}$$

In order to only generate the first-order and the second-order Stokes' wave, and suppress the higher-order Stokes' waves, the suitable fiber Bragg gratings as mirrors of Fabry-Perot cavity should be chosen to reach good performance. At least, the FBG1 should be chosen precisely. Fig. 2 shows the reflected output powers of pump, the first-order and the second-order Stokes' wave as functions of the reflectivity of FBG1. The parameters of the photonic crystal fiber are as follows: Brillouin gain coefficient g_B is 5.0×10^{-11} m/W, the effective core area of photonic crystal fiber A_{eff} is $5.0\,\mu\text{m}^2$, the optical attenuation

coefficient α is 6 dB/km. The length of the Fabry-Perot cavity is 25 m. The reflectivities of FBGs are chosen as $R_{p0} = R_{s20} = R$, $R_{s10} = 0.75$; $R_{pL} = 0.95$, $R_{s1L} = 0.95$, $R_{s2L} = 0.95$, respectively. Here, as we intend to investigate the second-order Stokes' wave, the reflectivities of FBG1 at the pump wave and the second-order Stokes' wave are supposed the same. R_{s10} is chosen for higher reflection of the first-order Stokes' wave, and the input power in the simulation is 0.3 W. The theoretical result shows that to generate the microwave signal with the laser, it is better to choose the reflectivities of FBG1 of $R_{p0} = R_{s20} \approx 0.3$, which leads to the equal emission power of the pump wave and the second-order Stokes' wave, as shown in Fig. 2.

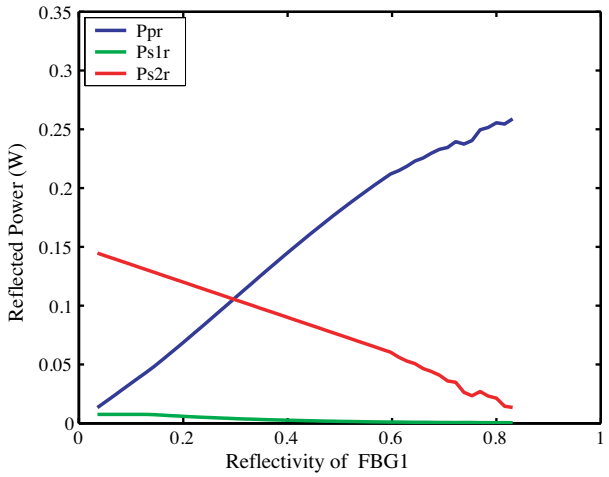

Figure 2. Reflected power as functions of the reflectivity of FBG1. Ppr, Ps1r and Ps2r are the powers of the pump, the first-order and the second-order Stokes' waves, respectively.

Figure 3 shows the reflected output powers of the pump wave, the first-order and the second-order Stokes' waves as functions of input power. In the calculation, the reflectivities of FBG1 are chosen as $R_{p0} = 0.43$, $R_{s10} = 0.75$, $R_{s20} = 0.32$, $R_{pL} = 0.95$, $R_{s1L} = 0.95$, $R_{s2L} = 0.95$, respectively.

3. EXPERIMENT AND RESULTS

Experiment setup for generating 9.788 GHz and 19.579 GHz microwave signals based on photonic crystal fiber Brillouin laser is shown in Fig. 4. The pump source is a tunable laser followed by an erbium-

doped fiber amplifier (EDFA). The linewidth of the tunable laser is about 100 kHz. The circulator is used to launch the pump into the photonic crystal fiber and extract the Stokes' wave. An approximately 25 m length photonic crystal fiber is used as Brillouin gain medium.

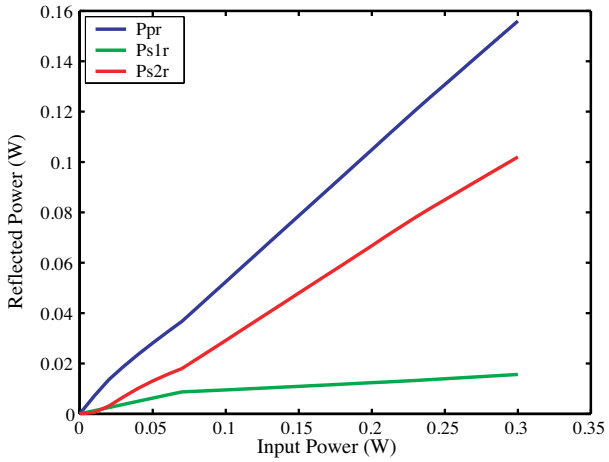

Figure 3. Output powers as functions of input power. Ppr, Ps1r and Ps2r are the power of the pump, the first-order and the second-order Stokes' waves, respectively.

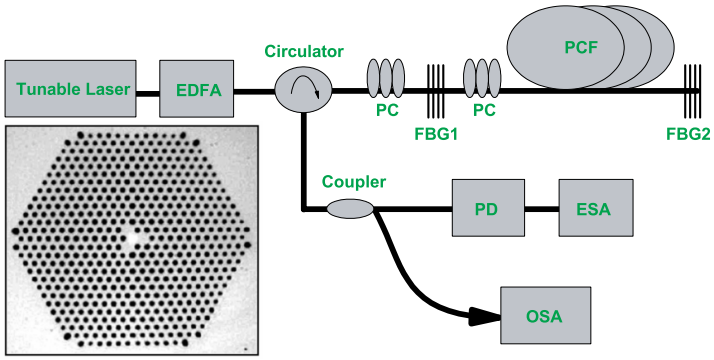

Figure 4. Experimental setup for microwave signal generation using Bragg grating Fabry-Perot cavity based photonic crystal fiber Brillouin laser. EDFA: erbium-doped fiber amplifier; PC: polarization controller; FBG: fiber Bragg grating; PCF: photonic crystal fiber; PD: photodetector; ESA: electronic spectrum analyzer; OSA: optical spectrum analyzer.

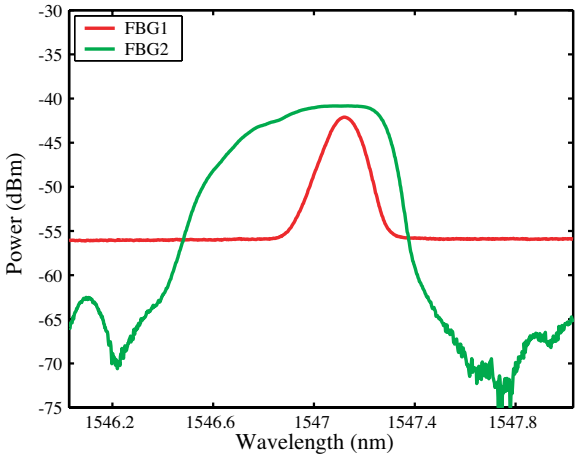

Figure 5. The reflection spectra of the two fiber Bragg gratings used in the experiment.

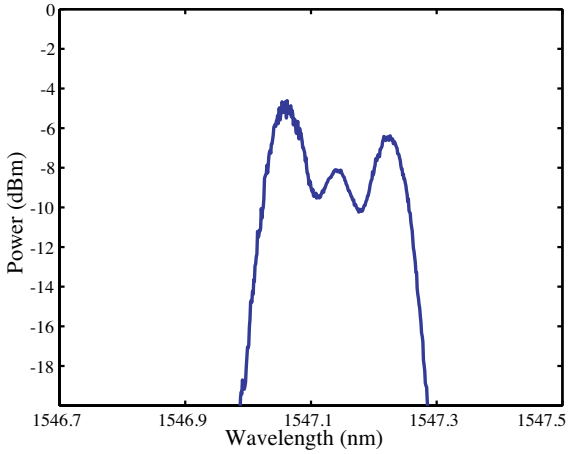

Figure 6. The output spectrum of the laser based at the input power of 180 mW.

The photonic crystal fiber is produced by Denmark Crystal Fiber A/S, which has parameters as follows: small mode field diameter at 1550 nm is about 2.5 μm, nonlinear coefficient at 1550 nm is about 11 $(\mathrm{WKm})^{-1}$, cladding diameter is about 125 μm, the optical attenuation coefficient is less than 9 dB/km at $1510 \sim 1620$ nm. The geometry of the fiber is shown in the inset of Fig. 4. The Brillouin shift frequency f_B of the

photonic crystal fiber is about 9.8 GHz. The reflection spectra of two FBGs used in the experiment are shown in Fig. 5. The reflectivities of FBGs used here are $R_{p0} = 0.43$, $R_{s10} = 0.75$, $R_{s20} = 0.32$, $R_{pL} = 0.95$, $R_{s1L} = 0.95$, $R_{s2L} = 0.95$, respectively. By stretching the FBGs, their center wavelengths can be tuned to the wavelength of the Stokes' wave. A polarization controller (PC1) before FBG1 is used to control the polarization of the input pump wave. Another polarization controller (PC2) in the fiber Fabry-Perot cavity is used to adjust the polarization of Stokes' waves to get maximum amplification and good stability of the laser. The laser output spectrum is analyzed with an optical spectrum analyzer (OSA). The output of the laser is then launched into a 60 GHz bandwidth photodetector (PD) after attenuation. The photodetector here is used to mix the reflected first-order or the second-order Stokes' waves with the pump wave, and then we can find microwave signals on the electronic spectrum analyzer (ESA), which has a upper limit of 26.5 GHz.

In the experiment, the wavelength of pump wave is set to 1547.06 nm, and the Stokes' waves at wavelength of 1547.142 nm and 1547.225 nm are found. When the input pump wave is amplified to about 50 mW, the stimulated Brillouin scattering occurs in the fiber Fabry-Perot cavity. The threshold is much lower than that needed in standard single mode fiber with the same system, which is almost 100 mW. It is shown that the stimulated Brilliouin scattering is much easier to occur in photonic crystal fiber than in standard single mode fiber. When the input pump wave increases to about 120 mW, the first-order Stokes' wave reaches the threshold, and the second-order Stokes' wave appears. Fig. 6 shows the output optical spectrum of the Brillouin laser at an input power of 180 mW. The laser output is detected by the photodetector. Two microwave signals of 9.788 GHz and 19.579 GHz are then attained as shown in Fig. 7. The signal shown in Fig. 7(a) is generated by mixing the first-order Stokes' wave and the pump wave, the signal shown in Fig. 7(b) is generated by mixing the second-order Stokes' wave and the pump wave. The bandwidth (full-width at half-maximum, or FWHM) of the two signals are 13.5 MHz and 8.5 MHz, respectively. We also make a test to use a segment of standard single mode fiber (SMF28) as Brillouin gain medium. Fig. 8 shows the output optical spectrum of the Brillouin laser with the single mode fiber at the input power of 180 mW. Two microwave signals of 10.879 GHz and 21.763 GHz of this laser are shown in Fig. 9. The FWHM of the signals are 7.5 MHz and 9 MHz, respectively.

From Fig. 6 and Fig. 8, it can be seen that as the attenuation coefficient of the photonic crystal fiber (about 9 dB/km at 1510 $\sim$ 1620 nm) is much higher than that of the single mode fiber

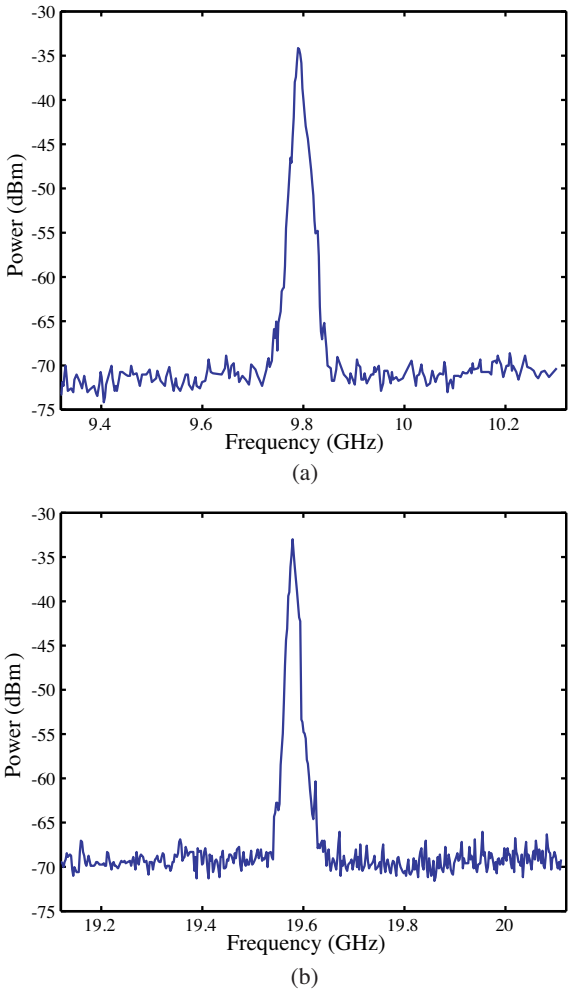

Figure 7. Microwave signals generated by the Brillouin laser.

(0.2 dB/km), the output power of Fig. 6 is a little lower. However, compared with the output power of the second-order Stokes' wave, the first-order Stokes' wave shown in Fig. 6 is much lower than that in Fig. 8. The reason is that the photonic crystal fiber has higher nonlinearity, which causes more power of the first-order Stokes' wave transferred into the second-order Stokes' wave, and makes the first-order signal weak. It is proved that the simulated Brillouin scattering is much easier to occur in the photonic crystal fiber than in the single mode fiber. The higher-order Stokes' wave can be attained with lower

input pump power based on the photonic crystal fiber, which also means that the Brillouin laser based on the photonic crystal fiber has higher conversion efficiency.

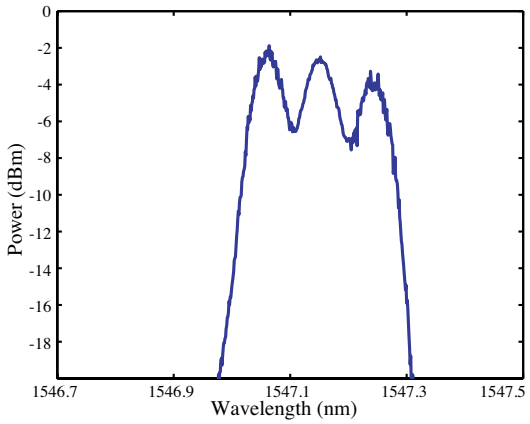

Figure 8. The output spectrum of the laser based on single mode fiber (SMF28) at the input power of 180 mW.

Since the temperature of the fiber will affect the Brillouin shift frequency and the frequency stability of the laser, we keep the temperature at room temperature during the experiment. It is necessary to note that the laser system here is treated with the assumption that the pump light always kept at resonance. In fact, when the pump wavelength is not resonant with the cavity, the pump power fades, so do the Stokes' waves. In our experiment, as the Fabry-Perot cavity length is a little longer, the freedom spectrum range is larger than the bandwidth of Brillouin gain (about 30 MHz), so that the laser works in multi-longitudinal mode, and generates more noise, which makes the phase noise of the microwave signals. Axial fluctuations in the holey fiber cross-sectional profile and the loss of fiber Bragg gratings, fiber splice loss and high transmission loss of the photonic crystal fiber also reduce the laser output power and the microwave signals power. A high-spectral-purity microwave can be obtained by using a narrower pump laser, or using ultra-narrow phase-shifted fiber Bragg grating instead of FBG1 [4].

The experiment results show that using the photonic crystal fiber as the Brillouin medium of the laser can lower the Brillouin threshold, and generate the high-order Stokes' wave easier than using the standard single mode fiber. With the rapid development of photonic crystal fiber technique, if the optical attenuation coefficient and splice loss of photonic crystal fiber can be reduced greatly, the performance of the photonic crystal fiber Brillouin laser will be improved a lot. By selecting more suitable fiber Bragg gratings, we can generate much higher and purer microwave and millimeter wave.

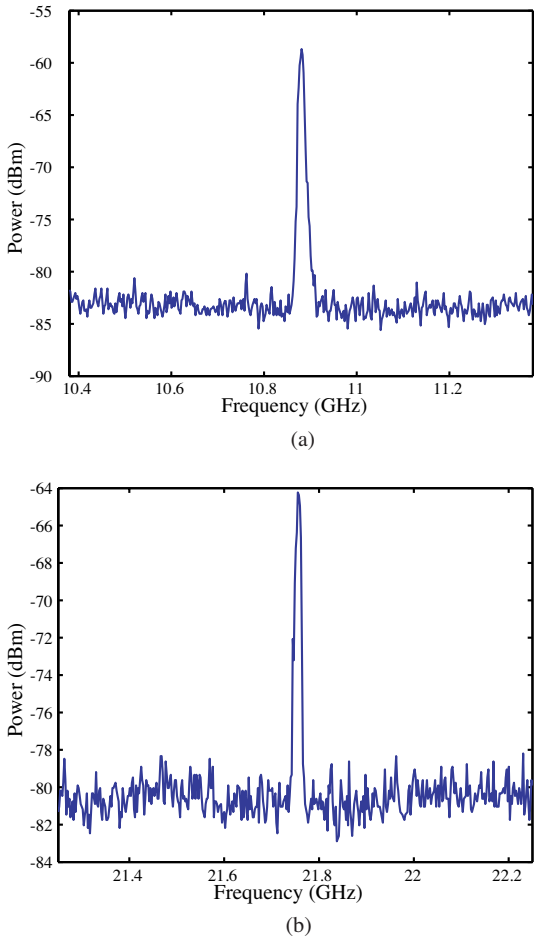

Figure 9. Microwave signal generated by the Brillouin laser based on single mode fiber (SMF28).

4. CONCLUSION

In summary, a technique for microwave/millimeter-wave signal generation using a multi-wavelength Fabry-Perot cavity laser based on photonic crystal fiber is investigated. By selecting suitable fiber Bragg gratings to form the fiber Fabry-Perot cavity, we can selectively excite the higher-order Stokes' waves. A microwave up to a millimeter-wave signal can be achieved by mixing the pump wave with the higher-order Stokes' wave. The first-order Stokes' wave and the second-order Stokes'

wave are excited in the experiment and two microwave signals at 9.788 GHz and 19.579 GHz are attained based on the photonic crystal fiber. The Brillouin threshold in the photonic crystal fiber with higher nonlinearity is lower than that in the standard single mode fiber. It is easier to excite the high-order Stokes' waves, and therefore to generate microwave/millimeter-wave.

ACKNOWLEDGMENT

This research was supported by National Natural Science Foundation of China (grant No. 60577028, 60407011, and 60471030), the Program for New Century Excellent Talents in University (No. NCET-05-518), and the Specialized Research Fund for the Doctoral Program of Higher Education of China (grant No. 20060335074).

REFERENCES

1. Qiao, S., T. Jiang, L. X. Ran, and K. S. Chen, "Ultra-wide band noise-signal radar utilizing microwave chaotic signals and chaos synchronization," *PIERS Online*, Vol. 3, No. 8, 1326–1329, 2007.
2. Georgiadou, E. M., A. D. Panagopoulos, and J. D. Kanellopoulos, "Millimeter wave pulse propagation through distorted raindrops for los fixed wireless access channels," *J. of Electromagn. Waves and Appl.*, Vol. 20, No. 9, 1235–1248, 2006.
3. Osipov, A. V., I. T. Iakubov, A. N. Lagarkov, S. A. Maklakov, D. A. Petrov, K. N. Rozanov, and I. A. Ryzhikov, "Multi-layered Fe films for microwave applications," *PIERS Online*, Vol. 3, No. 8, 1303–1306, 2007.
4. Bindu, G., A. Lonappan, V. Thomas, C. K. Aanandan, and K. T. Mathew, "Dielectric studies of corn syrup for applications in microwave breast imaging," *Progress In Electromagnetics Research*, PIER 59, 175–186, 2006.
5. Ku, H. S., "Productivity improvement of composites processing through the use of industrial microwave technologies," *Progress In Electromagnetics Research*, PIER 66, 267–285, 2006.
6. Pourova, M. and J. Vrba, "Analytical solutions to the applicatiors for microwave textile drying by means of zigzag method," *PIERS Online*, Vol. 3, No. 8, 1204–1207, 2007.
7. Bauer, S., O. Brox, J. Kreissl, G. Sahin, and B. Sartorius, "Optical microwave source," *Electron. Lett.*, Vol. 38, No. 7, 334–335, 2002.

8. Biswas, B. N., "Optical generation of mm-wave signal with wide linewidth lasers for broadband communications," *PIERS Online*, Vol. 3, No. 7, 1058–1063, 2007.
9. Biswas, B. N., A. Banerjee, A. Mukherjee, and S. Kar, "Lightwave technique of mm-wave generation for broadband mobile commmunication," *PIERS Online*, Vol. 3, No. 7, 1071–1075, 2007.
10. Hyodo, M., K. S. Abedin, N. Onodera, and M. Watanabe, "Beat-signal synchronization for optical generation of millimetre-wave signals," *Electron. Lett.*, Vol. 39, No. 24, 1740–1741, 2003.
11. Wu, J. W. and F. G. Luo, "Generation of high repetition rate picosecond pulse train based on ultra-small silicon waveguide," *Progress In Electromagnetics Research*, PIER 75, 163–170, 2007.
12. Brunel, M., F. Bretenaker, S. Blanc, V. Crozatier, J. Brisset, T. Merlet, and A. Poezevara, "High-spectral purity RF beat note generated by a two frequency solid-state laser in a dual thermooptic and electrooptic phaselocked loop," *IEEE Photon. Technol. Lett.*, Vol. 16, No. 3, 870–872, 2004.
13. Meng, X. J. and J. Menders, "Optical generation of microwave signals using SSB-based frequency-doubling scheme," *Electron. Lett.*, Vol. 39, No. 1, 103–105, 2003.
14. Sun, J., Y. T. Dai, X. F. Chen, Y. J. Zhang, and S. Z. Xie, "Stable dual-wavelength DFB fiber laser with separate resonant cavities and its application in tunable microwave generation," *IEEE Photon. Technol. Lett.*, Vol. 18, No. 24, 2587–2589, 2006.
15. Leng, J. S., Y. C. Lai, W. Zhang, and J. A. R. Williams, "A new method for microwave generation and data transmission using DFB laser based on fiber Bragg gratings," *IEEE Photon. Technol. Lett.*, Vol. 18, No. 16, 1729–1731, 2006.
16. Kitayama, K. I., "Highly stabilized millimeter wave generation by using fiber-optic frequency-tunable comb generator," *J. Lightw. Technol.*, Vol. 15, No. 5, 883–893, 1997.
17. Deng, Z. C. and J. P. Yao, "Photonic generation of microwave signal using a rational harmonic mode-locked fiber ring laser," *IEEE Trans. Microw. Theory Tech.*, Vol. 54, No. 2, 763–767, 2006.
18. Chen, X. F., Z. C. Deng, and J. P. Yao, "Photonic generation of microwave signal using a dual-wavelength single-longitudinal-mode fiber ring laser," *IEEE Trans. Microw. Theory Tech.*, Vol. 54, No. 2, 804–809, 2006.
19. Schneider, T., M. Junker, and D. Hannover. "Generation of millimetre-wave signals by stimulated Brillouin scattering for

radio over fibre systems," *Electron. Lett.*, Vol. 40, No. 23, 1500–1502, 2004.

20. Smith, S. P., F. Zarinetchi, and S. Ezekiel, "Narrow-linewidth stimulated Brillouin fiber laser and applications," *Opt. Lett.*, Vol. 16, No. 6, 393–395, 1991.
21. Yao, X. S., "High-quality microwave signal generation by use of brillouin scattering in optical fibers," *Opt. Lett.*, Vol. 22, No. 17, 1329–1331, 1997.
22. Shen, Y. C., X. M. Zhang, and K. S. Chen, "All-optical generation of microwave/millimeter-wave using a two-frequency Bragg grating based Brillouin fiber laser," *J. Lightw. Technol.*, Vol. 23, No. 5, 1860–1865, 2005.
23. Shen, Y. C., X. M. Zhang, and K. S. Chen, "Optical single sideband modulation of 11-GHz RoF system using stimulated Brillouin scattering," *IEEE Photon. Technol. Lett.*, Vol. 17, No. 6, 1277–1279, 2005.
24. Guenneau, S., A. Nicolet, F. Zolla, and S. Lasquellec, "Numerical and theoretical study of photonic crystal fibers," *Progress In Electromagnetics Research*, PIER 41, 271–305, 2003.
25. Song, W., Y. Y. Zhao, Y. Bao, S. G. Li, Z. Y. Zhang, and T. F. Xu, "Numerical simulation and analysis on mode property of photonic crystal fiber with high birefringence by fast multipole method," *PIERS Online*, Vol. 3, No. 6, 836–841, 2007.
26. de Matos, C. J. S., J. R. Taylor, and K. P. Hansen, "All-fibre Brillouin laser based on holey fibre yielding comb-like spectra," *Opt. Commun.*, Vol. 238, No. 1–3, 185–189, 2004.
27. Singh, S. P., R. Gangwar, and N. Singh, "Nonlinear scattering effects in optical fibers," *Progress In Electromagnetics Research*, PIER 74, 379–405, 2007.
28. Crutcher, S., A. Biswas, M. D. Aggarwal, and M. E. Edwards, "Oscillatory behavior of spatial solitons in tow-dimensional waveguides and stationary temporal power law solitons in optical fibers," *J. of Electromagn. Waves and Appl.*, Vol. 20, No. 6, 761–772, 2006.
29. Singh, S. P. and N. Singh, "Nonlinear effects in optical fibers: Origin, management, and applications," *Progress In Electromagnetics Research*, PIER 73, 249–275, 2007.
30. Ogusu, K., "Analysis of steady-state cascaded stimulated Brillouin scattering in a fiber Fabry-Perot resonator," *IEEE Photon. Technol. Lett.*, Vol. 14, No. 7, 947–949, 2002.